Acta Pharmacologica Sinica

www.nature.com/aps

ARTICLE

Caffeic acid phenethyl ester suppresses intestinal FXR signaling and ameliorates nonalcoholic fatty liver disease by inhibiting bacterial bile salt hydrolase activity

Xian-chun Zhong[1,2], Ya-meng Liu[2], Xiao-xia Gao[3], Kristopher W. Krausz[3], Bing Niu[1], Frank J. Gonzalez[3] and Cen Xie[2,3]

Propolis is commonly used in traditional Chinese medicine. Studies have demonstrated the therapeutic effects of propolis extracts and its major bioactive compound caffeic acid phenethyl ester (CAPE) on obesity and diabetes. Herein, CAPE was found to have pharmacological activity against nonalcoholic fatty liver disease (NAFLD) in diet-induced obese mice. CAPE, previously reported as an inhibitor of bacterial bile salt hydrolase (BSH), inhibited BSH enzymatic activity in the gut microbiota when administered to mice. Upon BSH inhibition by CAPE, levels of tauro-β-muricholic acid were increased in the intestine and selectively suppressed intestinal farnesoid X receptor (FXR) signaling. This resulted in lowering of the ceramides in the intestine that resulted from increased diet-induced obesity. Elevated intestinal ceramides are transported to the liver where they promoted fat production. Lowering FXR signaling was also accompanied by increased GLP-1 secretion. In support of this pathway, the therapeutic effects of CAPE on NAFLD were absent in intestinal FXR-deficient mice, and supplementation of mice with C16-ceramide significantly exacerbated hepatic steatosis. Treatment of mice with an antibiotic cocktail to deplete BSH-producing bacteria also abrogated the therapeutic activity of CAPE against NAFLD. These findings demonstrate that CAPE ameliorates obesity-related steatosis at least partly through the gut microbiota-bile acid-FXR pathway via inhibiting bacterial BSH activity and suggests that propolis enriched with CAPE might serve as a promising therapeutic agent for the treatment of NAFLD.

Keywords: nonalcoholic fatty liver disease; caffeic acid phenethyl ester; bile salt hydrolase; farnesoid X receptor; ceramide; gut microbiota

Acta Pharmacologica Sinica (2023) 44:145–156; https://doi.org/10.1038/s41401-022-00921-7

INTRODUCTION

Nonalcoholic fatty liver disease (NAFLD), given its increased prevalence in recent years that may replace chronic viral hepatitis as the top chronic liver disease, has led to a substantial clinical demand for new anti-NAFLD drugs [1]. NAFLD, that includes a broad range of pathologic changes, with the most common lesion being steatosis, may evolve into nonalcoholic steatohepatitis (NASH) and cirrhosis [2]. The "multiple parallel hits" theory is considered a better hypothesis to define the development of severe NAFLD and NASH. Although genetic susceptibility, innate immunity, oxidative stress, and endoplasmic reticulum stress were identified as combined risk factors, hepatic steatosis is still regarded as the first biochemical change that leads to NASH [3]. To date, there is a lack of FDA-approved drugs to treat the progression from obesity-related simple steatosis to NASH [4]. Therefore, it is necessary to find a novel therapeutic target and potential agents for NAFLD treatment.

Recent evidence suggests that regulation of farnesoid X receptor (FXR) signaling has beneficial effects on obesity [5]. FXR, expressed primarily in the liver and intestine, is a nuclear receptor that plays an essential role in controlling the synthesis, transport and enterohepatic circulation of bile acids (BA) [6]. Some conjugated BAs produced in the liver were identified as FXR antagonists, such as tauro-β-muricholic acid (T-β-MCA), glycoursodeoxycholic acid (G-UDCA), and tauroursodeoxycholic acid (T-UDCA) [7, 8]. Antagonism of intestinal FXR signaling ameliorates obesity-related metabolic dysfunction through the intestine-liver axis mediated by ceramide production from FXR target genes. Therefore, inhibition of intestinal FXR signaling is considered a potential target to treat NAFLD [9].

The gut microbiota can participate in many of the hosts metabolic processes, affecting nutrient uptake and energy harvest [10]. In the metabolic syndrome scenario, BA disorders are all likely related to compositional changes in the gut microbiota [11]. Bile salt hydrolase (BSH), produced by intestinal microbiota, is involved in BA metabolism in the host intestine. BSH hydrolyzes glycine- or taurine-conjugated BAs to non-conjugated BAs. The genera *Bacteroides*, *Lactobacillus*, and *Clostridium* express highly active BSH [12]. Hence, oral BSH inhibitors showed potential for the treatment of metabolic diseases through regulation of intestinal

[1]School of Life Sciences, Shanghai University, Shanghai 200444, China; [2]State Key Laboratory of Drug Research, Shanghai Institute of Materia Medica, Chinese Academy of Sciences, Shanghai 201203, China and [3]Laboratory of Metabolism, Center for Cancer Research, National Cancer Institute, National Institutes of Health, Bethesda 20892 Maryland, USA

Correspondence: Frank J. Gonzalez (gonzalef@mail.nih.gov) or Cen Xie (xiecen@simm.ac.cn)

These authors contributed equally: Xian-chun Zhong, Ya-meng Liu

Received: 13 March 2022 Accepted: 10 May 2022
Published online: 2 June 2022

FXR signaling by altering microbial function and reducing depolymerization of BAs [13, 14].

Propolis from beehives, a traditional Chinese medicine (TCM) that has been widely used over a long period of time, possesses a wide range of biological properties, such as antimicrobial, anti-inflammatory, antioxidant, and antitumor activities [15]. China and Brazil are the two major suppliers of raw propolis, even though the products are quite different in their botanical origins. The pharmacologically-active ingredients in propolis include flavonoids and phenolic acids and their esters. Different from the primary phenolic acids in Brazilian green propolis, Chinese propolis generally consists of a high caffeic acid phenethyl ester (CAPE) content, reaching 15–29 mg/g [16]. Propolis is now used as an over-the-counter dietary supplement and a natural source of the active compound CAPE, to support the immune system and hepatic health. Some studies demonstrated that CAPE reduces diet-induced metabolic syndrome and hepatic gluconeogenesis in mice [13, 17]. However, the therapeutic effects and underlying mechanism of CAPE on NAFLD are not fully understood. Importantly, CAPE was identified as a potent inhibitor of bacterial BSH [18]. The current study revealed that the administration of CAPE significantly ameliorates obesity-associated liver steatosis by targeting the BSH-intestinal FXR axis to reduce intestinal ceramides and increase GLP-1 secretion. CAPE treatment also improved gut dysbiosis. These findings suggest a novel role for BSH inhibitors in the prevention and treatment of NAFLD.

MATERIALS AND METHOD

Reagents and materials

CAPE was purchased from Bachem Americas, Inc. (Torrance, CA). d5-TCDCA and d5-CDCA sodium salt were obtained from Toronto Research Chemicals, Inc. (Toronto, Ontario). Bile acid metabolites were purchased from Sigma-Aldrich (St. Louis, MO) and Steraloids, Inc. (Newport, RI). Ceramides (C16:0, C18:0, C20:0, C22:0, C24:0, and C24:1) were purchased from Avanti Polar Lipids (Alabaster, AL). High-fat diet (HFD, 60 kcal% fat) was obtained from Bio-Serv, Inc. (S3282, Frenchtown, NJ) and Research Diets Inc. (D12492, New Brunswick, NJ), respectively.

Animal studies

Wild-type mice, $Fxr^{fl/fl}$ mice and intestine-specific *Fxr*-null ($Fxr^{\Delta IE}$) mice were on a C57BL/6 genetic background. $Fxr^{fl/fl}$ and $Fxr^{\Delta IE}$ male mice were backcrossed for more than 10 generations [19]. Six- to eight-week-old male littermate mice were kept on a 12-h light-dark cycle and fed ad libitum. All mice were randomly assigned to either the experimental or control groups, and there was no difference in body weights between the groups prior to dosing. The natural propolis prescribed to diabetic patients was reported at 1.0–2.5 $g \cdot kg^{-1} \cdot d^{-1}$ [20]. Through dose conversion, the propolis dose for mice was calculated at 10–25 $g \cdot kg^{-1} \cdot d^{-1}$, while the CAPE content in propolis is around 10%, equivalent to 100–250 mg/kg in mice [16]. In different studies, the doses of CAPE were reported to be around 75–100 mg/kg in mice [8, 21]. Taken together, a dose of 75 $mg \cdot kg^{-1} \cdot d^{-1}$ was chosen which is relevant to the clinical dose. CAPE was dissolved in dimethyl sulfoxide (DMSO) and diluted with saline to the desired concentration. All mouse experiments were conducted in accordance with the current guidelines of the Animal Ethics Committee of the Shanghai Institute of Materia Medica and the National Cancer Institute Animal Care and Use Committee.

For the prevention study, mice were divided into vehicle and CAPE-treated groups and fed a HFD (S3282) along with saline or CAPE (75 $mg \cdot kg^{-1} \cdot d^{-1}$) for 8 weeks. For therapeutic treatment, the mice were fed a HFD (D12492) for 8 weeks to establish hepatic steatosis, divided into NAFL-vehicle and NAFL-CAPE groups, and then administered saline or CAPE (75 $mg \cdot kg^{-1} \cdot d^{-1}$) for 8 weeks. In the intestinal FXR-dependent experiment, male 6- to 8-week-old $Fxr^{fl/fl}$ and $Fxr^{\Delta IE}$ mice under HFD feeding, were gavaged with saline or CAPE (75 $mg \cdot kg^{-1} \cdot d^{-1}$) for 8 weeks. For ceramide supplementation, $Fxr^{fl/fl}$ and $Fxr^{\Delta IE}$ mice fed a HFD were intraperitoneally injected with ceramide (C16:0, 10 mg/kg) suspended in 0.5% (*w/v*) sodium carboxymethyl cellulose or vehicle every two days for 5 weeks. For the gut microbiota depletion, mice fed a HFD were given an antibiotic cocktail (bacitracin, neomycin, and streptomycin) in drinking water at 0.1% (*w/v*) along with daily administration of saline or 75 mg/kg CAPE for 8 weeks. Food intake and body weights were monitored throughout the experiment. The experimental plan of the prevention study and FXR knockout study were similar to that described in a previous publication [13].

Body composition measurements

Body weight, lean and fat mass were measured using ^{1}H-NMR spectroscopy (Minispec LF90 II, Bruker, Germany) following manufacturer's protocol.

Triglyceride quantification

According to the manufacturer's recommendation, serum triglycerides were measured by a commercial assay kit (Bioassay Systems). For liver tissue, the samples were extracted using a 2:1 chloroform/methanol solution prior to quantification of the supernatant with the assay kit.

Histological analysis

Paraffin-embedded sections or frozen sections from the liver were stained with H&E or Oil red O according to standard protocols [22, 23]. Briefly, for H&E staining, the liver tissue was fixed for at least 24 h in 4% paraformaldehyde and then embedded with paraffin. Paraffin-embedded sections were then stained using hematoxylin-eosin. For Oil red O staining, the liver tissue was embedded in OCT, sectioned, and stained with Oil red O to visualize lipid droplets. The sections were then examined under a light microscope.

BSH activity assay

Measurement of BSH activity in the cecum contents was performed as described previously [24]. In brief, cecum contents were sonicated in cold phosphate-buffered saline (1:10, *w/v*), and then centrifuged to extract cecal protein. The assay system, including 10 μM d5-TCDCA and 0.1 mg/mL cecal protein, was incubated in 3 mM sodium acetate buffer (pH 5.2) at 37 °C for 20 min. The reaction was quickly terminated with an equal volume of ice-cold acetonitrile. After centrifugation, 20 μL of supernatant was mixed with 20 μL H_2O for further analysis.

GLP-1 measurements

GLP-1 concentrations were measured in the fed or glucose-stimulated state. For the glucose-stimulated state, the mice were fasted for 6 h and then gavaged with a single dose of sitagliptin (25 mg/kg). After 45 min, the mice received a single oral dose of glucose (2 g/kg). After 15 min, serum samples were collected to measure the levels of total and active GLP-1 using ELISA kit (Millipore, Bedford, MA).

Bile acids analysis

Ileal samples were prepared by precipitation with acetonitrile and then bile acid concentrations were measured using a Waters Synapt XS MS system (Waters Corporation, Milford, MA). Chromatographic separation was performed on a Waters Acquity BEH C18 column (2.1 × 100 mm) with a flow rate at 0.4 mL/min. The mobile phase A was 0.1% formic acid in H_2O and phase B was 0.1% formic acid in acetonitrile. The elution conditions were as described previously [9].

Quantification of ceramides

Serum and ileal samples were extracted with an ice-cold chloroform/methanol (2:1, *v/v*) solution containing ceramide C17:0 (Avanti Polar Lipids, Alabaster, AL) as an internal standard. The samples were incubated at 37 °C for 20 min with shaking and centrifuged at 14,000 r/min for 15 min. The lower organic phase was transferred to another tube and vacuum evaporated to dryness at room temperature. The evaporated samples were reconstituted in chloroform/methanol (1:1, *v/v*) and then diluted with isopropanol/acetonitrile/H_2O (2:1:1, *v:v:v*), followed by LC/MS analysis.

Lipidomics analysis was conducted on a Waters Xevo TQ MS. Samples were separated using a Waters Acquity BEH C column (2.1 × 100 mm). Mobile phase A was a H_2O/acetonitrile solution (containing 10 mM ammonium formate), while the mobile phase B was acetonitrile/isopropanol (containing 0.1% formic acid and 10 mM ammonium formate). The flow rate was 0.4 mL/min and the column temperature was maintained at 50 °C.

RNA extraction and qRT-PCR analysis

The intestine and liver tissues were snap-frozen in liquid nitrogen and stored at −80 °C until the RNAs were extracted. Total RNA was extracted from the tissues using TRIzol reagent (Invitrogen, Carlsbad, CA). RNA was converted to cDNA using PrimeScript reverse transcriptase (Takara Bio, Japan). qRT-PCR was conducted using SYBR Premix Ex Taq (Takara Bio, Japan) and a CFX384 real-time PCR detection system. The results were processed with the ΔΔCt method followed by normalization of the reference gene mRNAs. The sequences corresponding to the primers used in the study are shown in Supplementary Table 1.

16S rRNA gene sequencing

Fresh fecal samples were collected for 16S rRNA sequencing. Microbiota DNA was extracted by use of a fecal DNA isolation kit (QIAGEN, Düsseldorf, Germany). DNA was amplified using universal bacterial primers targeting the 16S rRNA variable V3-V4 region. The primers are shown in Supplementary Table 1. Amplification products were separated using a 2.0% agarose gel and purified using the QIAquick PCR purification kit (Qiagen, Valencia, CA). Bacterial DNA was sequenced on the Illumina HiSeq PE 150 platform and adapter-ligated DNA fragments were further sequenced according to standard protocols. UCLUST clustered the operational taxonomic units with 97% similarity. 16S rRNA gene sequencing analysis was performed as previously described [25].

Data analysis

All experimental data are presented as mean ± SD. Statistical analyses were processed with Student's *t*-test in GraphPad Prism (GraphPad Software, La Jolla, CA). *P* values < 0.05 * or #; <0.01 ** or ##; <0.001 *** or ###. Two-tailed Student's *t*-test was used to determine whether the data from the two groups were statistically different.

RESULTS

CAPE treatment ameliorates the development of NAFLD

To investigate whether CAPE could prevent NAFLD, HFD was used to induce obesity-related steatosis (Fig. 1a). Compared with the vehicle-treated group, CAPE treatment significantly prevented body mass gain and decreased fat mass and the fat/lean index (Fig. 1b–d). The decreased liver weight, liver weight (% body mass), and hepatic triglyceride levels, suggested that hepatic steatosis was also alleviated by CAPE treatment (Fig. 1e–h). These data were consistent with reduced lipid accumulation as seen in liver sections (Fig. 1i). In line with these data, the mRNA expression levels of hepatic sterol regulatory element binding protein-1c (*Srebp1c*) mRNA and its downstream target genes encoding cell death-inducing DFFA like effecter A (*Cidea*), fatty acid synthase (*Fasn*), acetyl-CoA carboxylase 1 (*Acc1*), elongases of very long-chain fatty acids (*Elovl*), fatty acid-binding protein 4 (*Fabp4*), stearoyl-CoA desaturase 1 (*Scd1*), and *Cd36,* were significantly suppressed (Fig. 1j). These data indicated that hepatic fatty acid *de novo* synthesis was affected after CAPE treatment.

To further determine whether CAPE intervention could decrease established steatosis, mice were fed a HFD for 8 weeks to induce steatosis and then treated with CAPE for an additional 8 weeks (Fig. 1k). Compared with the NAFL-V group, CAPE treatment was effective in controlling body mass gain as well as reducing fat mass and the fat/lean index in NAFLD mice (Fig. 1l–n). Liver weight, liver weight (% body mass), and hepatic triglyceride were significantly reduced after CAPE treatment, which is consistent with the above results that CAPE treatment decreases lipid accumulation (Fig. 1o–r). H&E and Oil red O staining of liver sections showed that hepatic steatosis and lipid droplet accumulation in mice was effectively decreased by CAPE treatment (Fig. 1s). At the mRNA level, hepatic lipogenesis-related and inflammatory factor-related genes were significantly decreased after CAPE treatment. These included *Acc1*, *Scd1*, and *Cd36* (lipid synthesis related), and the mRNAs encoding tumor necrosis factor alpha (*Tnfa*), interleukin 1 beta (*IL1β*), plasminogen activator inhibitor type 1 (*Pai1*), NLR family pyrin domain containing 3 (*Nlrp3*) (inflammation related) (Fig. 1t–u). Collectively, these results showed that CAPE intervention is capable of preventing and reversing NAFLD.

CAPE treatment inhibits BSH activity and modulates bile acid composition

CAPE is a potent inhibitor of BSH as identified by in vitro high-throughput screening [18]. To demonstrate the effect of CAPE on BSH in vivo, BSH activity was measured in cecum contents based on the enzymatic rate of d5-TCDCA deconjugated to d5-CDCA. As predicted, CAPE treatment markedly decreased BSH activity in cecum contents (Fig. 2a, b). These results indicated that reduced BSH activity altered the bile acid composition after CAPE treatment. To further explore the modification of ileal BAs, the composition of BAs after CAPE treatment was analyzed. Compared with the vehicle-treated group, the CAPE-treated group had increased ileal concentrations and percentages relative to total BAs of the endogenous FXR antagonist T-β-MCA, (Fig. 2c, d). In contrast, the percentages relative to total BAs of taurocholic acid (TCA) and taurodeoxycholic acid (T-DCA), known endogenous FXR agonists, were significantly decreased in CAPE-treated mice (Fig. 2d). Consistently, the expression of *Fxr* mRNA and its target gene mRNAs, fibroblast growth factor 15 (*Fgf15*) and small heterodimer partner (*Shp*), were decreased in ileum but not in liver after CAPE administration (Fig. 2e, f). Oral treatment with CAPE markedly induced ileal levels of the mRNA encoding proglucagon-1 (*Gcg*) encoding a precursor protein that is cleaved to form GLP-1 (Fig. 2e). Ceramide synthesis, which responds to FXR activation in intestinal epithelial cells, was further investigated in the ileum, revealing that CAPE inhibited *de novo* ceramide synthesis in mice due to lower serine palmitoyltransferase subunit 2 (*Sptlc2*), and ceramide synthase 2 and 4 (*Cers2, Cers4*) mRNAs (Fig. 2g). Collectively, these results suggested that CAPE indirectly downregulates intestinal FXR signaling via inhibiting bacterial BSH activity to increase the endogenous FXR antagonist T-β-MCA thereby reducing ileal ceramide synthesis and inducing GLP-1 release.

Inhibition of intestinal FXR signaling by CAPE ameliorates NAFLD

To further evaluate the role of intestinal FXR in the effect of CAPE treatment on NAFLD, HFD-fed control ($Fxr^{fl/fl}$) mice and intestine-specific *Fxr* knockout ($Fxr^{\Delta IE}$) mice were treated with CAPE. CAPE protected $Fxr^{fl/fl}$ mice from HFD-induced body mass gain but had

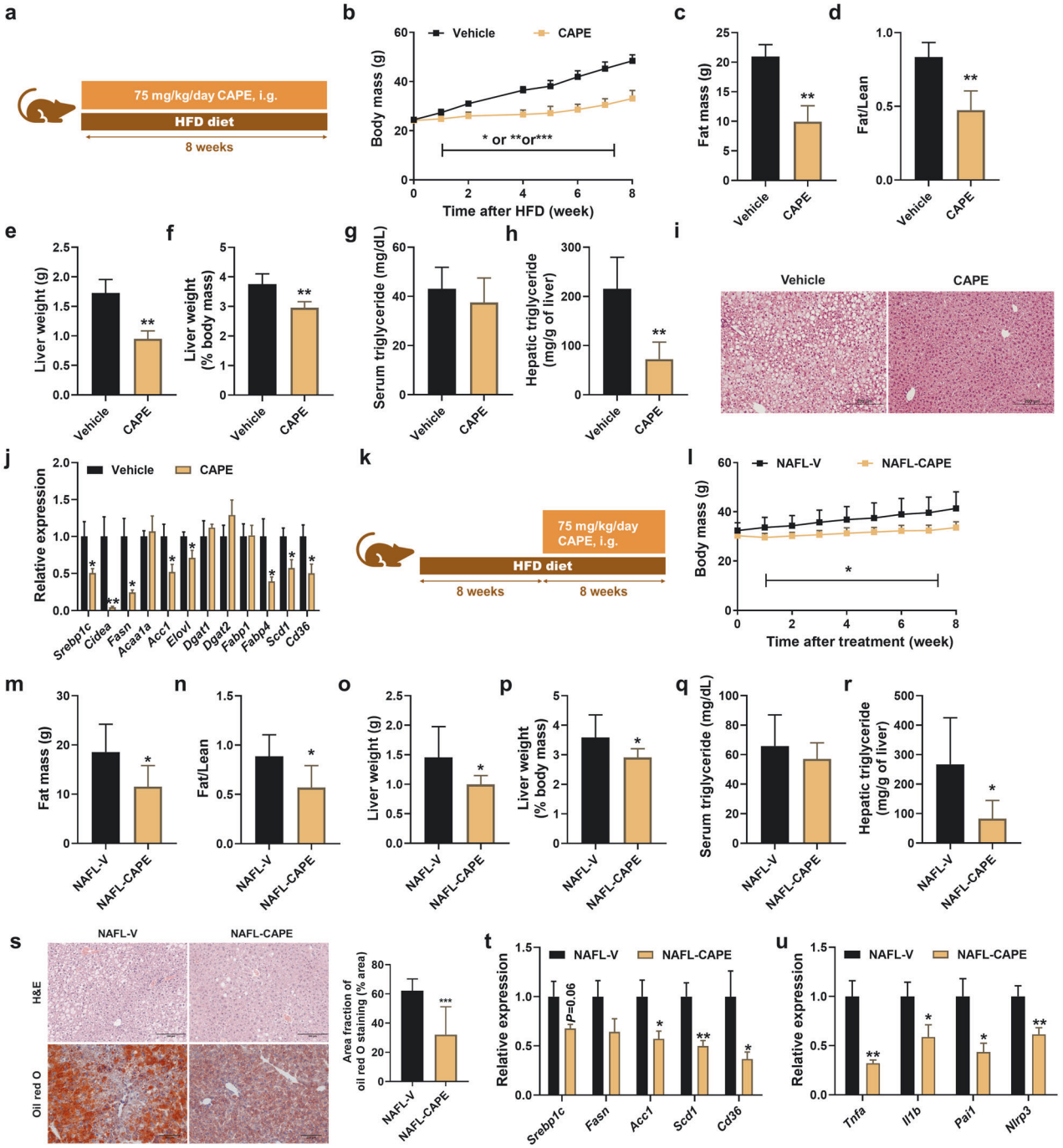

Fig. 1 CAPE ameliorated HFD-induced NAFLD. a Schematic diagram of CAPE for the prevention of NAFLD ($n = 5$). **b** Body mass. **c** Fat mass. **d** Fat/Lean index. **e** Liver weight. **f** Liver weight (% body mass). **g** Serum triglyceride. **h** Hepatic triglyceride. (**i**) Representative H&E staining of liver sections. **j** mRNA levels of the lipogenesis-related genes in liver. **k** Schematic diagram of CAPE for the intervention of NAFLD established steatosis ($n = 7$). **l** Body mass. **m** Fat mass. **n** Fat/Lean index. **o** Liver weight. **p** Liver weight (% body mass). **q** Serum triglyceride. **r** Hepatic triglyceride. **s** Representative H&E and Oil red O staining of liver sections. Lipids were stained positive (red color) with Oil red O and quantified by Image J software. **t** mRNA levels of the lipogenesis-related genes in liver. (**u**) mRNA levels of the inflammation-related genes in liver. Data are presented as the means ± SD. Two-tailed Student's *t*-test: $^{*}P < 0.05$, $^{**}P < 0.01$ and $^{***}P < 0.001$.

no effect on $Fxr^{\Delta IE}$ mice (Fig. 3a). Fat mass and fat/lean index were significantly decreased in CAPE-treated $Fxr^{fl/fl}$ mice compared with vehicle-treated $Fxr^{fl/fl}$ mice. However, $Fxr^{\Delta IE}$ mice showed no response to the anti-obesity benefits of CAPE administration (Fig. 3b, c). The decreased liver weight, liver weight (% body mass), and hepatic triglyceride indicated that CAPE substantially alleviated lipid accumulation in $Fxr^{fl/fl}$ mice whereas it did not affect $Fxr^{\Delta IE}$ mice (Fig. 3d–g). Furthermore, decreased levels of *Srebp1c*, *Cidea*, *Fasn*, *Acaa1a*, *Acc1*, *Elovl*, *Fabp4*, *Scd1*, and *Cd36* mRNAs revealed that hepatic lipogenesis was inhibited in CAPE-treated $Fxr^{fl/fl}$ mice. However, no further inhibition was observed in CAPE-treated $Fxr^{\Delta IE}$ mice compared with vehicle-treated $Fxr^{\Delta IE}$ mice (Fig. 3h). The morphology of reduced lipid accumulation in liver sections was only observed in CAPE treated $Fxr^{fl/fl}$ mice (Fig. 3i). However, total and individual taurine-conjugated bile acid levels showed the similar changes in CAPE-treated $Fxr^{\Delta IE}$ mice

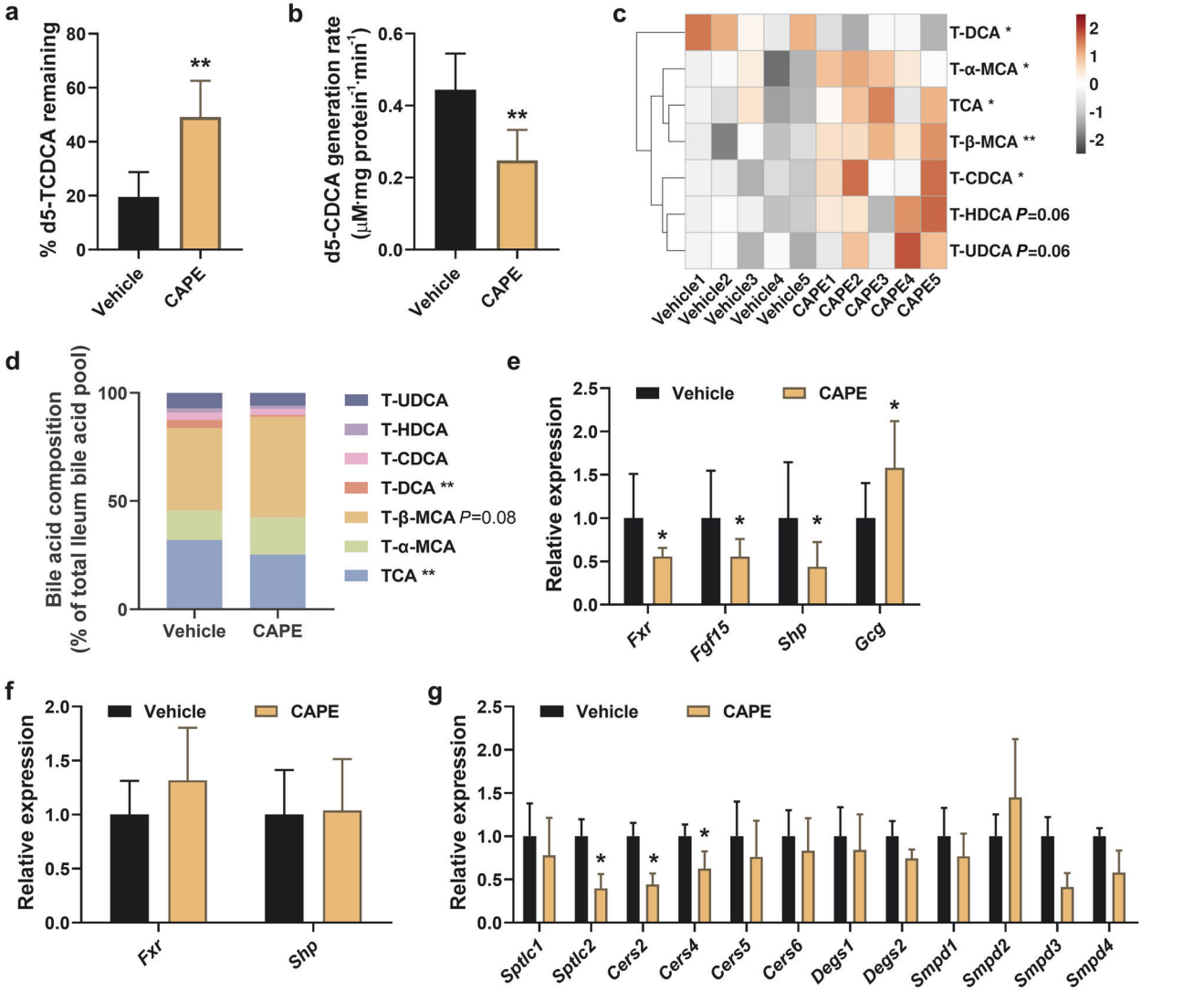

Fig. 2 CAPE treatment inhibits the BSH activity, regulates bile acid composition and inhibits intestinal FXR signaling. C57BL/6 mice fed a HFD treated with vehicle and CAPE for 8 weeks ($n = 5$). BSH enzymatic activity in the cecum contents as measured by the percentage of d5-TCDCA remaining **a** and the d5-CDCA generation rate **b** in the BSH incubations. The concentration (**c**) and percentage (**d**) of the individual taurine-conjugated BAs in ileum. mRNA levels of FXR target genes (*Fxr*, *Fgf15* and *Shp*) and *Gcg* in the ileum. **f** mRNA levels of FXR target genes (*Fxr*, and *Shp*) in liver. **g** mRNA levels for ceramide synthesis-related enzymes in the ileum. Data are presented as the means ± SD. Two-tailed Student's *t*-test: $^{*}P < 0.05$ and $^{**}P < 0.01$.

(Fig. S1a–c), which supported an essential role for BA remodeling that results from CAPE treatment.

CAPE treatment reduces ceramide levels and promotes GLP-1 secretion in an FXR-dependent manner

Since synthesis of ceramides in ileum was changed after CAPE treatment (Fig. 2g), further studies were performed to determine whether ceramide levels decline in response to intestinal FXR modulation. Total ceramide levels were markedly decreased in serum and ileum of CAPE-treated $Fxr^{fl/fl}$ mice and vehicle-treated $Fxr^{\Delta IE}$ mice compared with vehicle-treated $Fxr^{fl/fl}$ mice, while no further decrease in total ceramide levels was observed in CAPE-treated $Fxr^{\Delta IE}$ mice (Fig. 4a, c). Furthermore, CAPE treatment altered the compositions of ceramides in serum and ileum, as shown by reduced C16:0, C18:0, C20:0, C22:0, and C24:0 in $Fxr^{fl/fl}$ mice, and no changes were found in $Fxr^{\Delta IE}$ mice (Fig. 4b, d).

One study reported that activation of FXR in intestinal L cells decreased glycolysis and ATP production, thereby reducing the expression of *Gcg* and GLP-1 production [26]. The present results showed that intestinal FXR deficiency also increased serum GLP-1 concentrations, consistent with increased *Gcg* mRNA in the ileum [26]. Total GLP-1 levels were increased in serum of CAPE-treated $Fxr^{fl/fl}$ mice and vehicle-treated $Fxr^{\Delta IE}$ mice compared with vehicle-treated $Fxr^{fl/fl}$ mice in the fed state, and active GLP-1 levels were also observed in the postprandial (fasted + glucose stimulation) state (Fig. 4e, f). These results suggested that CAPE treatment can reduce ceramide levels and promote GLP-1 secretion in an FXR-dependent manner.

Ceramide supplementation in intestinal FXR-deficient mice promotes NAFLD development

To further assess the role of intestine-derived ceramide in the regulation of intestinal FXR on hepatic lipogenesis, C16:0 ceramide was administered by intraperitoneal injection to $Fxr^{\Delta IE}$ mice fed a HFD. Compared to vehicle-treated $Fxr^{\Delta IE}$ mice, supplementation with ceramide eliminated the decreased body weight gain in vehicle-treated $Fxr^{\Delta IE}$ mice (Fig. 5a). Consequently, the changes in fat mass (Fig. 5b) and fat/lean index (Fig. 5c) were reversed after

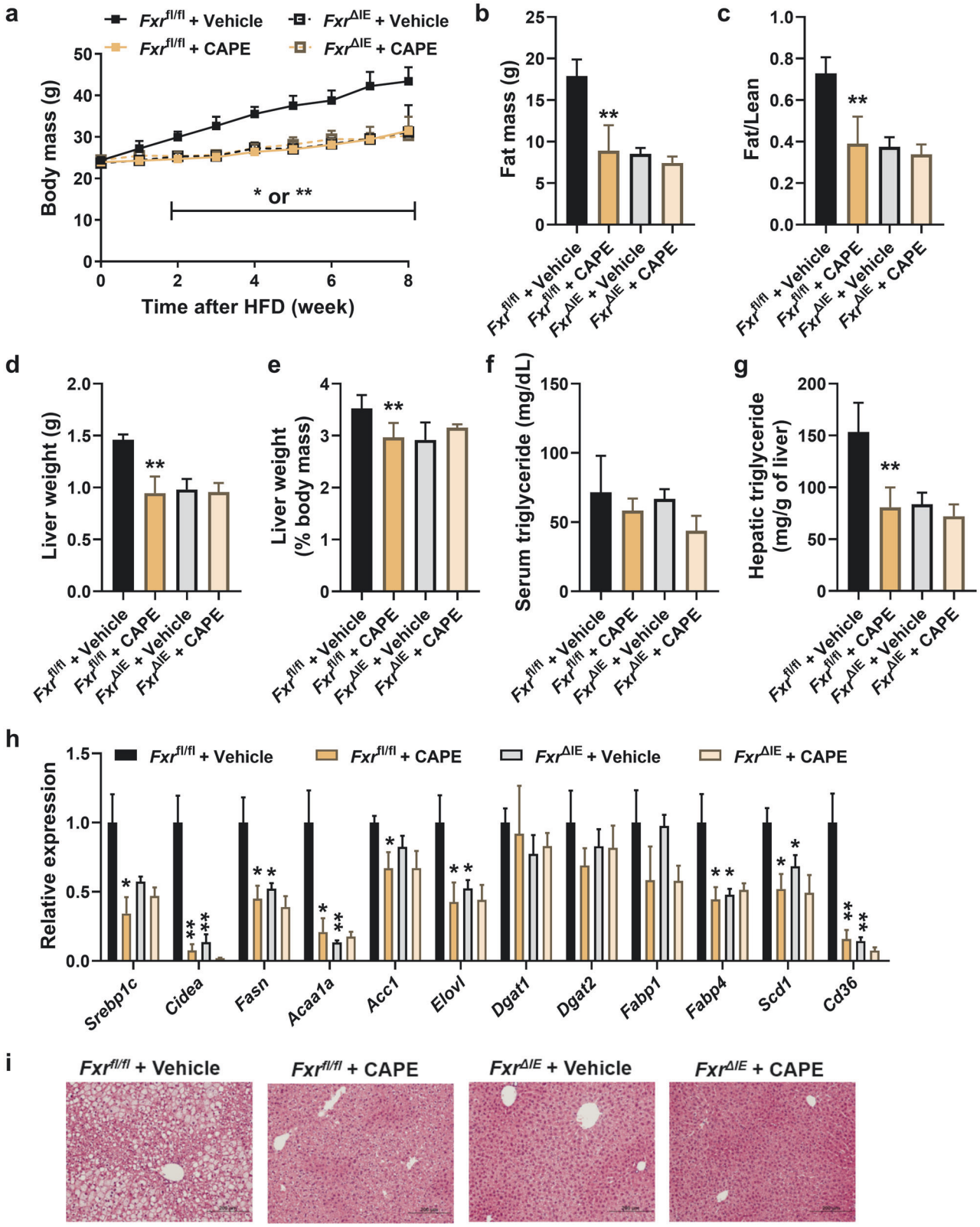

Fig. 3 Inhibition of intestinal FXR is necessary to improve NAFLD by CAPE. $Fxr^{fl/fl}$ mice and intestine-specific *Fxr* knockout ($Fxr^{\Delta IE}$) mice fed a HFD were treated with vehicle or CAPE for 8 weeks ($n = 5$). **a** Body mass. **b** Fat mass. **c** Fat/lean index. **d** Liver weight. **e** Liver weight (% body mass). **f** Serum triglyceride. **g** Hepatic triglyceride. (**h**) mRNA levels of the lipogenesis-related genes in liver. (**i**) Representative H&E staining of liver sections. Data are presented as the means ± SD. Compare with $Fxr^{fl/fl}$ + Vehicle. Two-tailed Student's *t*-test: $^{*}P < 0.05$, $^{**}P < 0.01$.

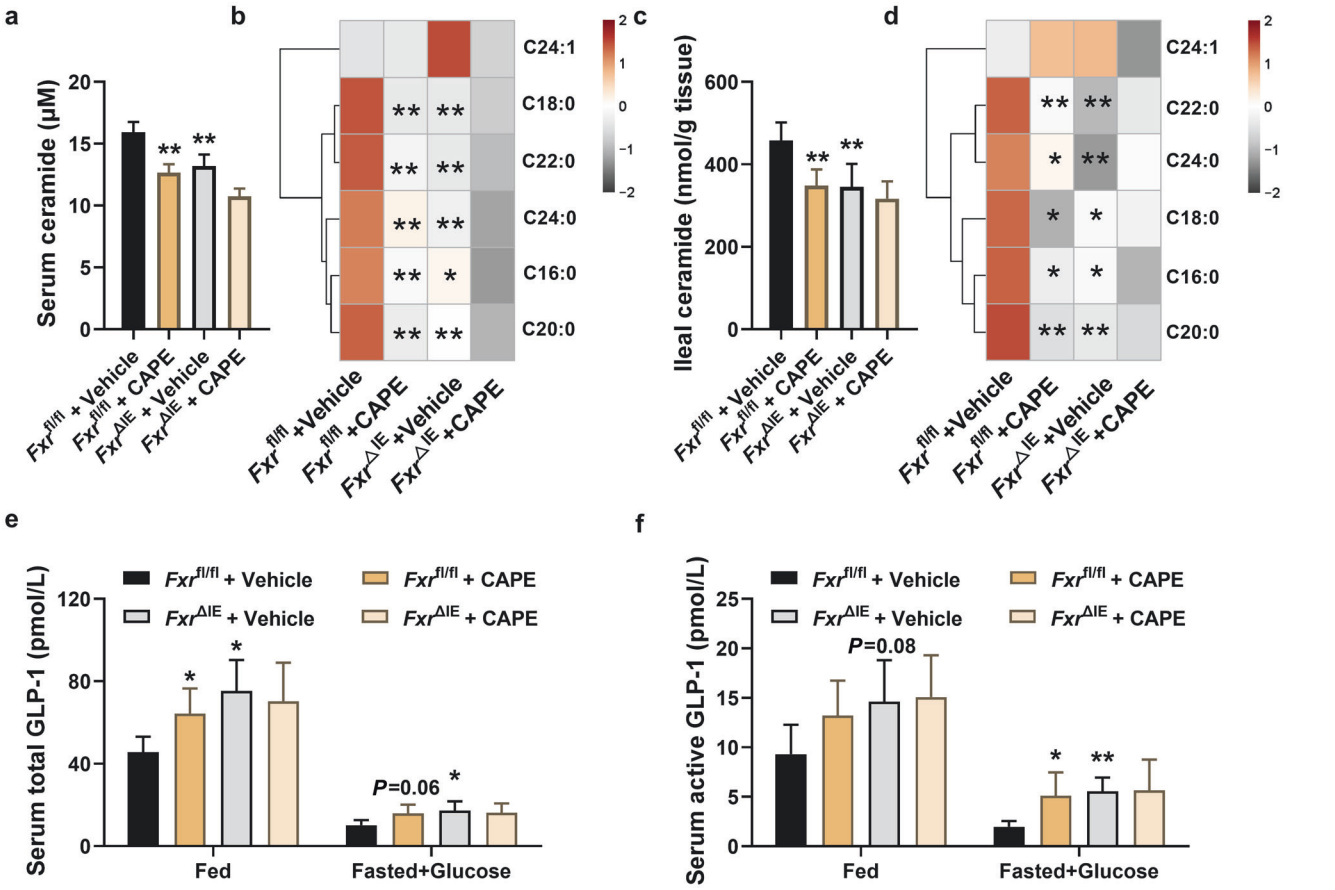

Fig. 4 Oral administration of CAPE reduces ceramide and promotes GLP-1 secretion. a The total serum ceramide levels in vehicle- and CAPE-treated *Fxr*$^{fl/fl}$ and *Fxr*$^{\Delta IE}$ mice after 8 weeks of HFD feeding ($n = 5$). **b** The individual serum ceramide levels in vehicle- and CAPE-treated *Fxr*$^{fl/fl}$ and *Fxr*$^{\Delta IE}$ mice after 8 weeks of HFD feeding ($n = 5$). **c** The total ileal ceramide levels in vehicle- and CAPE-treated *Fxr*$^{fl/fl}$ and *Fxr*$^{\Delta IE}$ mice after 8 weeks of HFD feeding ($n = 5$). **d** The individual ileal ceramide levels in vehicle- and CAPE-treated *Fxr*$^{fl/fl}$ and *Fxr*$^{\Delta IE}$ mice after 8 weeks of HFD feeding ($n = 5$). **e** The serum total GLP-1 in vehicle- or CAPE-treated *Fxr*$^{fl/fl}$ and *Fxr*$^{\Delta IE}$ mice in the fed or fasted plus glucose state ($n = 5$). **f** The serum active GLP-1 in vehicle- or CAPE-treated *Fxr*$^{fl/fl}$ and *Fxr*$^{\Delta IE}$ mice in the fed or fasted plus glucose state ($n = 5$). Data are presented as the means ± SD. Two-tailed Student's *t*-test: $^{*}P < 0.05$ and $^{**}P < 0.01$.

ceramide was replenished. Moreover, the results obtained from liver weight, hepatic triglyceride, mRNA expression of hepatic lipogenesis-related genes, and the morphology of liver sections (Fig. 5d–h), together indicated that the intestinal FXR disruption-mediated reduced hepatic lipogenesis was abolished by ceramide administration to *Fxr*$^{\Delta IE}$ mice. These data confirmed that intestinal synthesized ceramides could circulate to the liver and induce steatosis.

CAPE treatment ameliorates the development of NAFLD via gut microbiota remodeling

To verify the role of gut microbiota following CAPE-induced FXR inhibition, HFD-fed mice were treated with an antibiotic cocktail to determine the role of BSH-expressing microbiota in preventing the progression of NAFLD. After depleting the gut microbiota, the therapeutic effects of CAPE disappeared (Fig. 6a–i). After antibiotic intervention, oral administration of CAPE did not alter the taurine-conjugated bile acid composition (Fig. S2a, b). Antibiotic + CAPE treatment led to no change in ileum *Fxr* mRNA levels, FXR target gene mRNA levels, and ceramide-synthetic related gene mRNA levels (Fig. S2c, d). These results revealed that long-term CAPE treatment improves obesity-related steatosis through the intestinal FXR-ceramide axis in a manner dependent on BSH-producing microbes.

Next, the mechanism by which CAPE influenced gut microbiota compositions was investigated. Fecal samples harvested towards the endpoint of CAPE treatment were examined for bacterial community compositions by 16 S rRNA sequencing. CAPE decreased the OTU number and Chao1 index, indicating that CAPE reduced gut microbiota richness and diversity (Fig. S3a–d). PCA analysis showed a significant difference between vehicle and CAPE-treated mice (Fig. 7a). CAPE treatment altered the proportion of Firmicutes, Proteobacteria, and Actinobacteria at the phylum level, but no alterations in Bacteroidetes were noted (Fig. 7b, Fig. S3e–h). In addition, it was reported that BSH-producing bacteria belong to 117 genera of 12 phyla, and more than half of the BSH-producing bacteria belong to Firmicutes [27]. Therefore, the reduced abundance of Firmicutes may be due to BSH inhibition. At the genera level, CAPE treatment mainly increased *Bacteroides*, *Enterococcus*, *Bilophila* and *Helicobacter*; *Bacteroides* and *Enterococcus* were reported to be components of the majority of probiotics. The main decreased bacteria include *Intestinimonas*, *Lachnospiraceae*, *Parabacteroides*, *Faecalibacteium*, of which *Parabacteroides* are BSH-producing bacteria (Fig. 7c) [27]. At the species level (Fig. S3i, j), CAPE treatment led to enrichment of *Bacteroides acidifaciens* and *Lactobacillus coryniformis*, which were negatively associated with obesity [28, 29]. *Ruminococcus torques* and *Escherichia coli* were enriched in vehicle-treated mice. It is noteworthy that increased *Escherichia coli* were reported in overweight women [30]. These results suggested that CAPE can modulate intestinal microbiota structure, increase the abundance of probiotics and reduce the

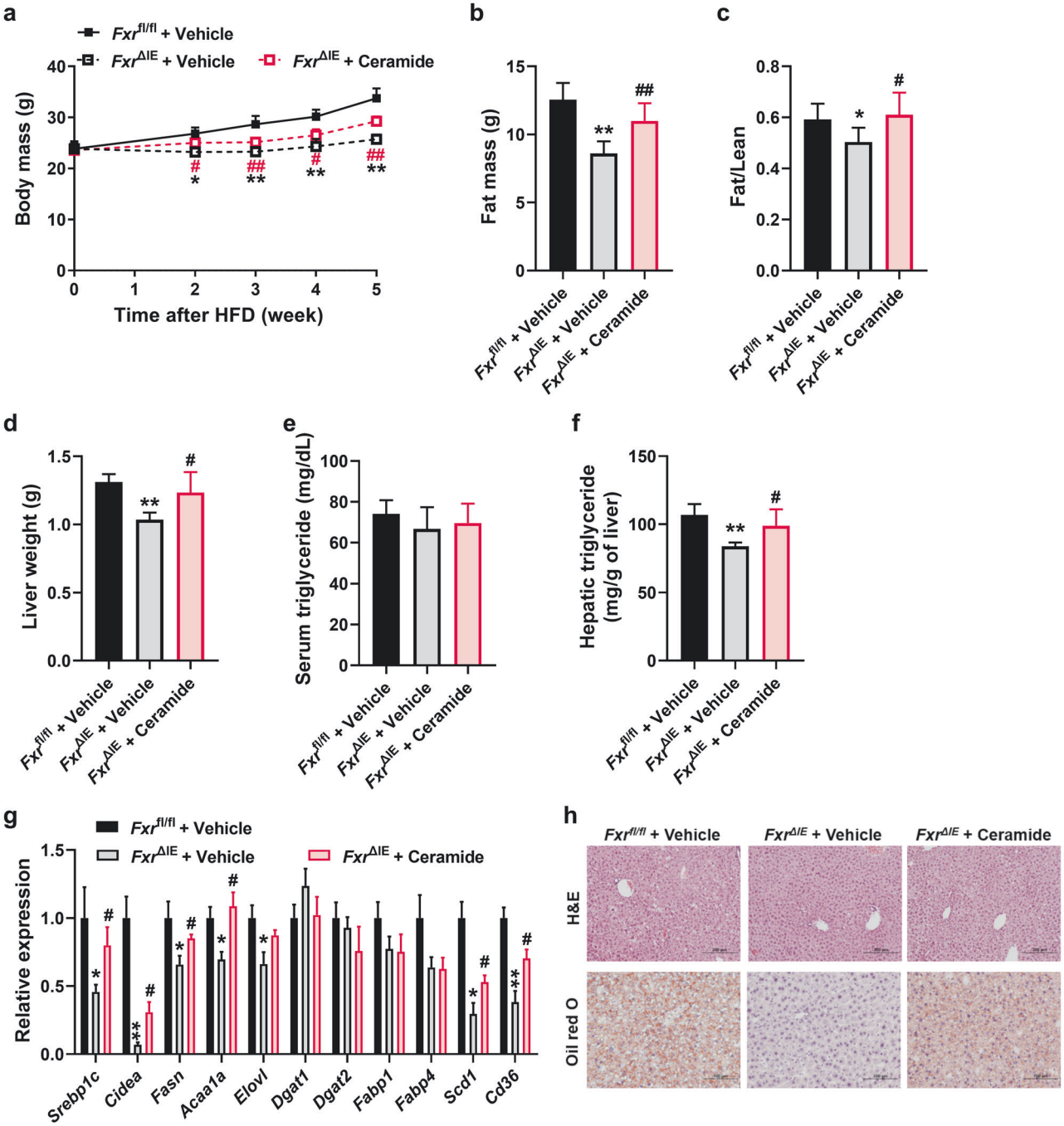

Fig. 5 Administration of ceramide reverses the benefit of intestinal FXR inhibition. $Fxr^{\Delta IE}$ mice fed a HFD were injected with or without ceramide for 5 weeks ($n = 5$). **a** Body mass. **b** Fat mass. **c** Fat/lean index. **d** Liver weight. **e** Serum triglyceride. **f** Hepatic triglyceride. **g** mRNA levels of the lipogenesis-related genes in liver. **h** Representative H&E staining and Oil red O staining of liver sections. Data are presented as the means ± SD. $Fxr^{fl/fl}$ + Vehicle vs $Fxr^{\Delta IE}$ + Vehicle: *, $Fxr^{\Delta IE}$ + Vehicle vs $Fxr^{\Delta IE}$ + Ceramide: #. Two-tailed Student's *t*-test: * or # $P < 0.05$, ** or ## $P < 0.01$.

abundance of BSH-producing bacteria and some harmful bacteria, thus improving NAFLD.

DISCUSSION

Recently, remarkable progress has been reported in TCM, an extensive and notable untapped resource for modern drug therapy, as exemplified by the antimalarial artemisinin [31]. CAPE, a phenolic compound with an ester bond, is cleaved by an esterase followed by rapid uptake into cells due to its high permeability. The CAPE content of propolis from different regions varies, with propolis from China having the highest CAPE content. To date, CAPE has been highlighted for its excellent therapeutic effects in endocrine and metabolic diseases [17], including hyperlipidemia, hypertension, and hyperglycemia, but there is limited knowledge on its effect on NAFLD. CAPE was identified by in vitro high-throughput screening as a potent BSH inhibitor [18]. However, the molecular mechanism by which CAPE affects NAFLD has not been investigated. Herein, the anti-NAFLD effects of CAPE were found to be associated with modulation of microbial BSH

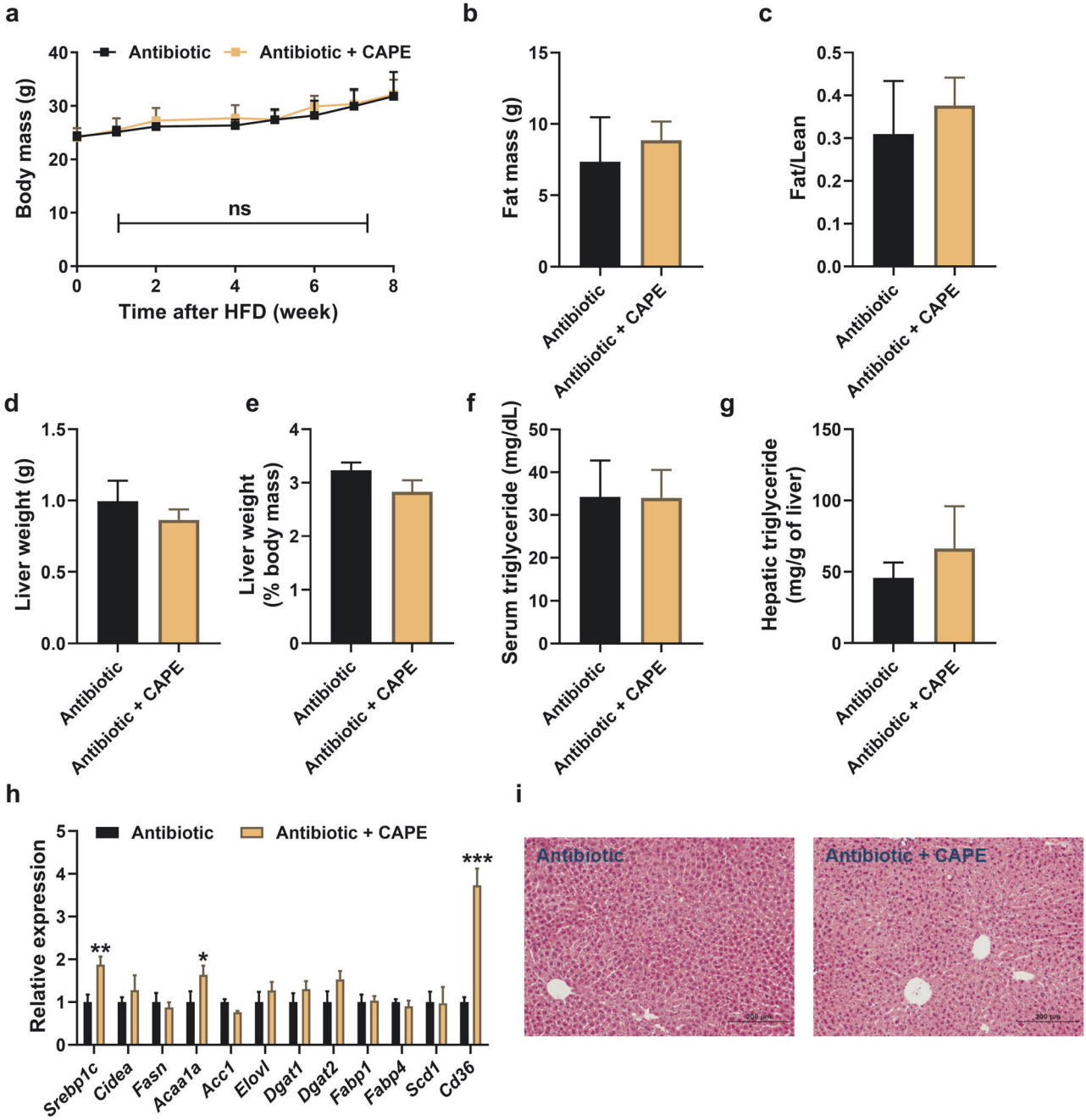

Fig. 6 Gut microbiota mediates the therapeutic effects of CAPE treatment. C57BL/6 mice fed a HFD treated with vehicle and antibiotic for 8 weeks ($n = 5$). **a** Body mass. **b** Fat mass. **c** Fat/lean index. **d** Liver weight. **e** Liver weight (% body mass). **f** Serum triglyceride. **g** Hepatic triglyceride. **h** mRNA levels of the lipogenesis-related genes in liver. **i** Representative H&E staining of liver sections. Data are presented as the means ± SD. Two-tailed Student's *t*-test: ns: no significant, $^{*}P < 0.05$, $^{**}P < 0.01$ and $^{***}P < 0.001$.

activity and inhibition of intestinal FXR signaling. Mechanistically, CAPE reduced obesity-related steatosis by decreasing intestinal ceramide synthesis, promoting GLP-1 secretion and lowering NAFLD (Fig. 8).

FXR, a bile acid-activated nuclear receptor, is highly expressed in the liver and intestine. FXR mediates crosstalk between these two organs and maintains bile acid homeostasis. FXR activation impaired cellular energy expenditure in the intestine and further potentiated obesity and imbalanced glucose metabolism, whereas genetic and pharmacological intestinal FXR inhibition produced metabolic advantages [13]. Although published evidence suggests that intestinal FXR controls intestinal ceramide synthesis, the precise mechanism by which ceramides stimulate hepatic steatosis remains elusive. The products of ceramide synthase (CERS) reactions, during *de novo* biosynthesis, are the dihydroceramides. The key step, catalyzed by CERS1-6, accounts for much of the diversity in sphingolipids by adding acyl chains to the sphingolipid scaffold [32]. Activation of intestinal FXR induced increased synthesis of ceramides that are transported to the liver where they stimulate steatosis [33]. In vitro, overexpression of CERS6 in primary hepatocytes was shown to be sufficient to increase levels of C16:0 ceramides that induce triglyceride accumulation and stimulate mitochondrial respiration injury [34]. C16:0 is the predominant form of intestinal ceramides. It enters

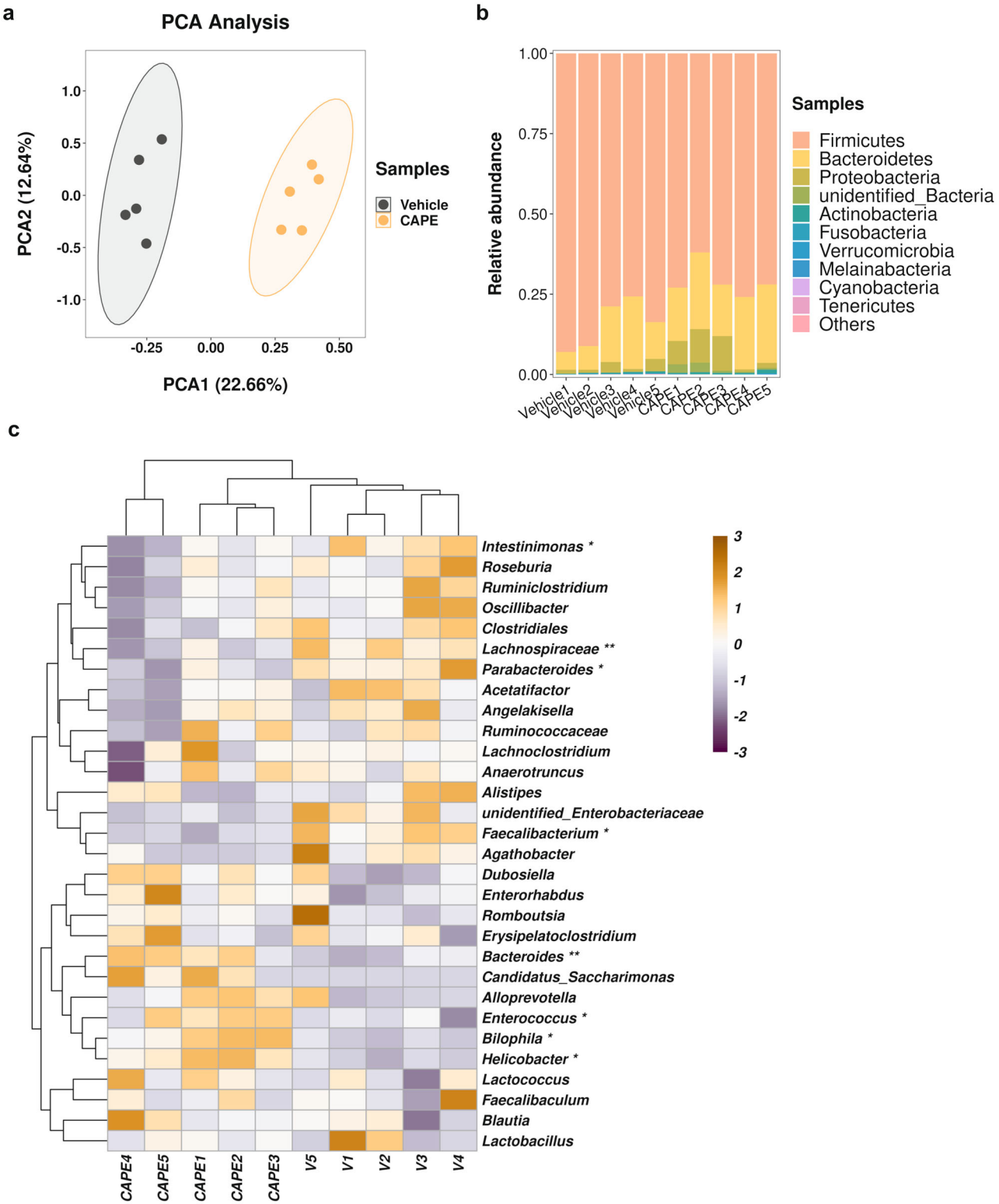

Fig. 7 CAPE alters the gut microbiota compositions. a PCA analysis. **b** Barplot of the relative abundance of gut microbiota at the phylum level. **c** The relative abundance of the microbiota in the feces at the genera level. Two-tailed Student's *t*-test: $^{*}P < 0.05$ and $^{**}P < 0.01$.

the hepatic portal vein after intraperitoneal administration which mimics the action of endogenous intestine-derived ceramides. Repeated ceramide injections raise the average ceramide levels to the approximate serum concentrations found in HFD-fed mice and induce NAFLD, obesity, and insulin resistance without inducing toxicity (data not shown). In the current study, the *de novo* pathway of ceramide synthesis-related genes, including *Sptlc2*, *Cers2*, and *Cers4*, was decreased after CAPE treatment and this was associated with inhibition of FXR signaling. A previous study investigated genome-wide FXR binding in the intestine of mice treated with the synthetic FXR ligand GW4064 by use of chromatin immunoprecipitation coupled to massively parallel sequencing

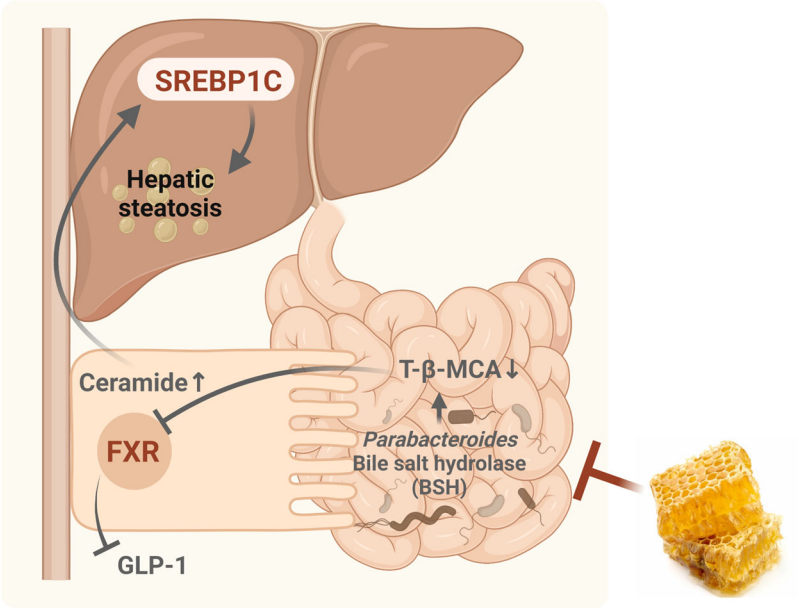

Fig. 8 Summary of the role of the BSH-intestinal FXR-ceramide axis in amelioration of NAFLD by CAPE treatment. Propolis from China contains the highest levels of CAPE, which can inhibit BSH activity by suppressing the abundance of BSH-producing bacteria such as *Parabacteroides*, after oral administration. Inhibition of BSH by CAPE leads to an increase in T-β-MCA, which in turn inhibits intestinal FXR signaling that decreases ceramide synthesis and promotes GLP-1 secretion. Ceramide enters the liver and stimulates lipid synthesis, induces hepatic steatosis, and potentiates NAFLD development. Therefore, CAPE may improve NAFLD by inhibiting bacterial BSH activity, altering bile acid compositions, and regulating the intestinal FXR signaling-ceramide axis.

(ChIP-seq) [35]. By analyzing the public data from this study, a prominent FXR binding peak was found in an intron of the *Cers2* gene.

The exact mechanism linking the gut microbiota to TCM can be divided into two aspects: (i) influence the growth of the microbial community and, hence, the bacterial profile, and (ii) target metabolizing enzymes in the gut microbiota, such as CAZyme, BSH, and baiH. Earlier animal and human studies have implicated disruption of gut microbial homeostasis in NAFLD [36, 37]. Therefore, remodeling the gut microbiota or altering their microbial functions are potentially effective strategies in managing NAFLD. Conjugated BAs play an essential role in lipid solubilization and are the target substrates of BSH. Modifying bacterial bile acid metabolism using a BSH inhibitor may represent a promising therapeutic strategy to treat NAFLD.

In the present work, CAPE treatment decreased the richness of the microbiota, especially the proportion of genera *Parabacteroides* that express high levels of BSH. Notably, the proportions of genera *Bacteroides* and *Enterococcus* were increased, which were reported as popular probiotics. Therefore, an upregulation of most conjugated bile acids by CAPE treatment was observed, except for T-DCA. Although BSH carries out the gateway reaction for bile acid metabolism, 7α-dehydroxylation is also an important part of the pathway that modifies cholic acid (CA) to produce the secondary bile acid deoxycholic acid (DCA). Several potential BSH expressing bacteria are capable of 7α-dehydroxylation, including Clostridia and *Eubacterium* [38]. Moreover, Lachnospiraceae, Ruminococcaceae, *Peptostreptococcus*, and Clostridiaceae are the confirmed 7α-dehydroxylase-active bacteria [39]. Consistently, CAPE treatment reduced the abundance of c_Clostridia, g_*Lachnospiraceae* and s_*Eubacterium hallii*, which hindered the biotransformation of primary bile acids to secondary bile acids and thus might contribute to the decreased T-DCA levels.

There are some limitations to the present study. First, CAPE can be hydrolyzed to CA. The serum levels of CA were higher than CAPE in CAPE-treated mice, and antibiotic intervention significantly lowered CA levels (data not shown). However, the serum concentration of CA is relatively low after CAPE treatment compared to the high CAPE dosage (75 mg/kg) employed and its relatively high exposure in the intestine. It should be noted that other mechanisms could be involved in the anti-NAFLD action of CAPE. Second, while the present study revealed a critical role for the gut microbiota during CAPE treatment, there is a lack of detail on how CAPE specifically inhibits bacterial BSH activity and selectively regulates intestinal FXR signaling. Third, while intestine FXR deficiency was associated with increased serum GLP-1 levels, an earlier study reported that TGR5 directly promotes GLP-1 secretion while FXR indirectly regulates GLP-1 secretion via a mechanism that depends on downstream TGR5 signaling [40–42]. Hence, the roles of TGR5 in CAPE-mediated *Gcg* and GLP-1 upregulation have not been completely clarified in the present work. More in-depth studies and mechanistic investigations are warranted.

In summary, the current study demonstrated that long-term administration of CAPE protected mice from HFD-induced obesity and ameliorated hepatic steatosis. Mechanistically, CAPE treatment inhibited BSH enzymatic activity, increased the proportions of T-β-MCA and decreased TCA and T-DCA in the intestine, which led to inhibition of FXR signaling and lower ceramide synthesis, while inducing GLP-1 secretion. The therapeutic effects of CAPE on NAFLD were absent in the intestinal FXR deficient mice, and supplementation of mice with C16:0 ceramide greatly potentiated hepatic steatosis. Depleting the gut microbiota by an antibiotic cocktail also eliminated BSH-expressing bacteria and the activity of CAPE against NAFLD. These findings confirmed that CAPE ameliorates obesity-related steatosis at least partly through the gut microbiota-intestinal FXR axis via inhibiting bacterial BSH activity. CAPE may serve as a promising natural therapeutic agent for NAFLD.

ACKNOWLEDGEMENTS

This work was supported by the grants from the National Key Research and Development Program of China (2021YFA1301200), National Natural Science

Foundation of China (91957116, 82104261), China Postdoctoral Science Foundation (2020M671269), Project supported by Shanghai Municipal Science and Technology Major Project, and the Intramural Research Program, Center for Cancer Research, National Cancer Institute, National Institutes of Health.

AUTHOR CONTRIBUTIONS

XCZ, YML, XXG, KWK, and CX conducted the experiments. XCZ, YML, and CX analyzed the data and wrote manuscript. CX, FJG, BN designed, supervised, and revised the manuscript.

ADDITIONAL INFORMATION

Supplementary information The online version contains supplementary material available at https://doi.org/10.1038/s41401-022-00921-7.

Competing interests: The authors declare no competing interests.

REFERENCES

1. Younossi Z, Anstee QM, Marietti M, Hardy T, Henry L, Eslam M, et al. Global burden of NAFLD and NASH: trends, predictions, risk factors and prevention. Nat Rev Gastroenterol Hepatol. 2018;15:11–20.
2. Baffy G, Brunt EM, Caldwell SH. Hepatocellular carcinoma in non-alcoholic fatty liver disease: an emerging menace. J Hepatol. 2012;56:1384–91.
3. Tilg H, Moschen AR. Evolution of inflammation in nonalcoholic fatty liver disease: the multiple parallel hits hypothesis. Hepatology. 2010;52:1836–46.
4. Friedman SL, Neuschwander-Tetri BA, Rinella M, Sanyal AJ. Mechanisms of NAFLD development and therapeutic strategies. Nat Med. 2018;24:908–22.
5. Jiang C, Xie C, Lv Y, Li J, Krausz KW, Shi J, et al. Intestine-selective farnesoid X receptor inhibition improves obesity-related metabolic dysfunction. Nat Commun. 2015;6:10166.
6. Jiang L, Zhang H, Xiao D, Wei H, Chen Y. Farnesoid X receptor (FXR): Structures and ligands. Comput Struct Biotechnol J. 2021;19:2148–59.
7. Sayin SI, Wahlström A, Felin J, Jäntti S, Marschall HU, Bamberg K, et al. Gut microbiota regulates bile acid metabolism by reducing the levels of tauro-beta-muricholic acid, a naturally occurring FXR antagonist. Cell Metab. 2013;133:225–35.
8. Sun L, Xie C, Wang G, Wu Y, Wu Q, Wang X, et al. Gut microbiota and intestinal FXR mediate the clinical benefits of metformin. Nat Med. 2018;24:1919–29.
9. Jiang C, Xie C, Li F, Zhang L, Nichols RG, Krausz KW, et al. Intestinal farnesoid X receptor signaling promotes nonalcoholic fatty liver disease. J Clin Invest. 2015;125:386–402.
10. Nicholson JK, Holmes E, Kinross J, Burcelin R, Gibson G, Jia W, et al. Host-gut microbiota metabolic interactions. Science. 2012;336:1262–7.
11. Wang PX, Deng XR, Zhang CH, Yuan HJ. Gut microbiota and metabolic syndrome. Chin Med J. 2020;133:808–16.
12. Bourgin M, Kriaa A, Mkaouar H, Mariaule V, Jablaoui A, Maguin E, et al. Bile salt hydrolases: at the crossroads of microbiota and human health. Microorganisms. 2021;9:1122.
13. Xie C, Jiang C, Shi J, Gao X, Sun D, Sun L, et al. An intestinal Farnesoid X receptor-ceramide signaling axis modulates hepatic gluconeogenesis in mice. Diabetes. 2017;66:613–26.
14. Xie Z, Jiang H, Liu W, Zhang X, Chen D, Sun S, et al. The triterpenoid sapogenin (2alpha-OH-Protopanoxadiol) ameliorates metabolic syndrome via the intestinal FXR/GLP-1 axis through gut microbiota remodelling. Cell Death Dis. 2020;11:770.
15. Bankova V, Boudourova-Krasteva G, Sforcin JM, Frete X, Kujumgiev A, Maimoni-Rodella R, et al. Phytochemical evidence for the plant origin of Brazilian propolis from São Paulo state. Z Naturforsch C J Biosci. 1999;54:401–5.
16. Lv L, Cui H, Ma Z, Liu X, Yang L. Recent progresses in the pharmacological activities of caffeic acid phenethyl ester. Naunyn Schmiedebergs Arch Pharmacol. 2021;394:1327–39.
17. Kim SH, Park HS, Hong MJ, Hur HJ, Kwon DY, Kim MS. Caffeic acid phenethyl ester improves metabolic syndrome by activating PPAR-γ and inducing adipose tissue remodeling in diet-induced obese mice. Mol Nutr Food Res. 2018;62:e1700701.
18. Smith K, Zeng X, Lin J. Discovery of bile salt hydrolase inhibitors using an efficient high-throughput screening system. PLoS One. 2014;9:e85344.
19. Kim I, Ahn SH, Inagaki T, Choi M, Ito S, Guo GL, et al. Differential regulation of bile acid homeostasis by the farnesoid X receptor in liver and intestine. J Lipid Res. 2007;48:2664–72.
20. Bahrami M, Ataie-Jafari A, Hosseini S, Foruzanfar MH, Rahmani M, Pajouhi M. Effects of natural honey consumption in diabetic patients: an 8-week randomized clinical trial. Int J Food Sci Nutr. 2009;60:618–26.
21. Ren J, Zhang N, Liao H, Chen S, Xu L, Li J, et al. Caffeic acid phenethyl ester attenuates pathological cardiac hypertrophy by regulation of MEK/ERK signaling pathway in vivo and vitro. Life Sci. 2017;181:53–61.
22. Feldman AT, Wolfe D. Tissue processing and hematoxylin and eosin staining. Methods Mol Biol. 2014;1180:31–43.
23. Davison PR, Cohle SD. Histologic detection of fat emboli. J Forensic Sci. 1987;32:1426–30.
24. Li F, Jiang C, Krausz KW, Li Y, Albert I, Hao H, et al. Microbiome remodelling leads to inhibition of intestinal farnesoid X receptor signalling and decreased obesity. Nat Commun. 2013;4:2384.
25. Lozupone C, Knight R. UniFrac: a new phylogenetic method for comparing microbial communities. Appl Environ Microbiol. 2005;71:8228–35.
26. Trabelsi MS, Daoudi M, Prawitt J, Ducastel S, Touche V, Sayin SI, et al. Farnesoid X receptor inhibits glucagon-like peptide-1 production by enteroendocrine L cells. Nat Commun. 2015;6:7629.
27. Song Z, Cai Y, Lao X, Wang X, Lin X, Cui Y, et al. Taxonomic profiling and populational patterns of bacterial bile salt hydrolase (BSH) genes based on worldwide human gut microbiome. Microbiome. 2019;7:9.
28. Yang JY, Lee YS, Kim Y, Lee SH, Ryu S, Fukuda S, et al. Gut commensal Bacteroides acidifaciens prevents obesity and improves insulin sensitivity in mice. Mucosal Immunol. 2017;10:104–16.
29. Toral M, Gómez-Guzmán M, Jiménez R, Romero M, Sánchez M, Utrilla MP, et al. The probiotic *Lactobacillus coryniformis* CECT5711 reduces the vascular pro-oxidant and pro-inflammatory status in obese mice. Clin Sci. 2014;127:33–45.
30. Santacruz A, Collado MC, García-Valdés L, Segura MT, Martín-Lagos JA, Anjos T, et al. Gut microbiota composition is associated with body weight, weight gain and biochemical parameters in pregnant women. Br J Nutr. 2010;104:83–92.
31. Klayman DL. Qinghaosu (artemisinin): an antimalarial drug from China. Science. 1985;228:1049–55.
32. Rahmaniyan M, Qudeimat A, MJ. Bioactive sphingolipids in neuroblastoma. In: Neuroblastoma - Present and Future. (2012), Chapter 8.
33. Gonzalez FJ, Jiang C, Patterson AD. An intestinal microbiota-farnesoid X receptor axis modulates metabolic disease. Gastroenterology. 2016;151:845–59.
34. Raichur S, Wang ST, Chan PW, Li Y, Ching J, Chaurasia B, et al. CerS2 haploinsufficiency inhibits β-oxidation and confers susceptibility to diet-induced steatohepatitis and insulin resistance. Cell Metab. 2014;20:687–95.
35. Thomas AM, Hart SN, Kong B, Fang J, Zhong XB, Guo GL. Genome-wide tissue-specific farnesoid X receptor binding in mouse liver and intestine. Hepatology. 2010;51:1410–9.
36. Li H, Wang Q, Chen P, Zhou C, Zhang X, Chen L. Ursodeoxycholic acid treatment restores gut microbiota and alleviates liver inflammation in non-alcoholic steatohepatitic mouse model. Front Pharmacol. 2021;12:788558.
37. Leung C, Rivera L, Furness JB, Angus PW. The role of the gut microbiota in NAFLD. Nat Rev Gastroenterol Hepatol. 2016;13:412–25.
38. Jukes CA, Ijaz UZ, Buckley A, Spencer J, Irvine J, Candlish D, et al. Bile salt metabolism is not the only factor contributing to Clostridioides (Clostridium) difficile disease severity in the murine model of disease. Gut Microbes. 2020;11:481–96.
39. Pi Y, Mu C, Gao K, Liu Z, Peng Y, Zhu W. Increasing the hindgut carbohydrate/protein ratio by cecal infusion of corn starch or casein hydrolysate drives gut microbiota-related bile acid metabolism to stimulate colonic barrier function. mSystems. 2020;5:e00176-20.
40. Pathak P, Liu H, Boehme S, Xie C, Krausz KW, Gonzalez F, et al. Farnesoid X receptor induces Takeda G-protein receptor 5 cross-talk to regulate bile acid synthesis and hepatic metabolism. J Biol Chem. 2017;292:11055–69.
41. Kapodistria K, Tsilibary EP, Kotsopoulou E, Moustardas P, Kitsiou P. Liraglutide, a human glucagon-like peptide-1 analogue, stimulates AKT-dependent survival signalling and inhibits pancreatic β-cell apoptosis. J Cell Mol Med. 2018;22:2970–80.
42. Pathak P, Xie C, Nichols RG, Ferrell JM, Boehme S, Krausz KW, et al. Intestine farnesoid X receptor agonist and the gut microbiota activate G-protein bile acid receptor-1 signaling to improve metabolism. Hepatology. 2018;68:1574–88.